A cluster variation approach to the random-anisotropy Blume-Emery-Griffiths model

1994 J. Phys.: Condens. Matter 6 327

(http://iopscience.iop.org/0953-8984/6/2/005)

J. Phys.: Condens. Matter 6 (1994) 327–338. Printed in the UK

A cluster variation approach to the random-anisotropy Blume–Emery–Griffiths model

Carla Buzano†, Amos Maritan‡ and Alessandro Pelizzola†

† Dipartimento di Fisica and Unitá INFM, Politecnico di Torino, I-10129 Torino, Italy

‡ Dipartimento di Fisica, Universitá di Padova and INFN Sez. di Padova, I-35131 Padova, Italy

Received 2 June 1993, in final form 11 October 1993

Abstract. The random-anisotropy Blume–Emery–Griffiths model, which has been proposed to describe the critical behaviour of ^{3}He–^{4}He mixtures in a porous medium, is studied in the pair approximation of the cluster variation method extended to disordered systems. Several new features, with respect to mean-field theory, are found, including a rich ground state, a non-zero percolation threshold, a reentrant coexistence curve and a miscibility gap on the high-^{3}He-concentration side down to zero temperature. Furthermore, nearest-neighbour correlations are introduced into the random distribution of the anisotropy, and are shown to be responsible for the raising of the critical temperature with respect to the pure and uncorrelated random cases and to contribute to the detachment of the coexistence curve from the λ line.

1. Introduction

The study of the effects of randomness on phase transitions has a long history and only recently has there been considerable experimental and theoretical effort to understand them in depth. Here we will be concerned with a simple model for the phase separation of ^{3}He–^{4}He mixtures in aerogel [1].

Aerogel is an extremely porous medium, the silica glass, made via the sol–gel process [2]. Its porosity may be as high as 99.8% [3] corresponding to a density of 4 mg cm^{-3}. There is experimental evidence [2, 4] that the aerogel microstructure is rather ramified, composed of silica strands with a thickness of the order of 10 Å and with an area of the order of 700 m^2 g^{-1} [5].

In order to describe in a simple way the effects of the porous medium on the phase separation diagram of ^{3}He–^{4}He we model the aerogel as a random external field that selects which of the two types of helium to have nearby. Thus it is quite interesting, among various other things, to understand the effect of the two types of impurity, i.e. the annealed ^{3}He and the quenched randomness of the external field, on the superfluid transition of ^{4}He.

Using mean-field theory, transfer-matrix and real-space renormalization group calculations it is possible to predict a variety of physically acceptable scenarios for the phase separation diagram as the density of the quenched impurities is varied [1]. The main features are the disappearance of the tricritical point present only in the pure ^{3}He–^{4}He system [6] and superfluidity in two coexisting phases, one rich in ^{3}He and the other in ^{4}He. Recent experiments [7] have confirmed the above qualitative picture.

The goal of this paper is to give a detailed study of the model proposed in [1] using the pair approximation of the cluster variation method (CVM) [8], generalized to random systems [9, 10]. This approximation improves the standard mean-field theory by taking into

0953-8984/94/020327+12$07.50

account effects of correlation among spins at different sites. Most of the qualitative features of the mean-field phase diagram are preserved.

Our approach allows us to incorporate effects of nearest-neighbour (NN) correlations in the quenched impurities, which are essential to a full understanding of the role of aerogel in the ^{3}He–^{4}He phase diagram. Unlike the coexistence curve, the λ line separating the normal fluid from the superfluid is rather sensitive to correlations of the quenched impurities at high ^{3}He concentration. Interesting new features are found in the $T = 0$ phase diagram and the role of the percolation threshold is elucidated.

In the next section the random-anisotropy Blume–Emery–Griffiths (RABEG) model will be introduced. The CVM generalized to random systems will be discussed in detail in connection with the RABEG model. Section 3 is devoted to the discussion of the phase diagram obtained in the present approximation, including connection with experimental results, and in section 4 some conclusions are drawn.

2. Definition of the model and the CVM pair approximation

The Blume–Emery–Griffiths (BEG) model [6] has been introduced as a model for ^{3}He–^{4}He mixtures, and subsequently applied to many other systems such as magnetic alloys and multicomponent fluids. It is a spin-1 system with NN interactions and a uniform-anisotropy external field distinguishing only between the ± 1 and 0 values of the spin. When dealing with ^{3}He–^{4}He mixtures [6] the ± 1 and 0 spin states represent ^{4}He and ^{3}He respectively, and the superfluid transition is associated with the spontaneous symmetry breaking between the ± 1 states. This is of course an approximation, since the superfluid transition of ^{4}He is in the XY class, and not in the Ising one, but nevertheless the model reproduces quite well the phase diagram of ^{3}He–^{4}He mixtures.

The generalization of the BEG model for a ^{3}He–^{4}He mixture in a porous medium is described by the Hamiltonian [1]

$$H = -J \sum_{\langle ij \rangle} S_i S_j - K \sum_{\langle ij \rangle} S_i^2 S_j^2 + \sum_i \Delta_i S_i^2 \tag{1}$$

where the spin variables $S_i = 0, \pm 1$ are defined on sites of a lattice Λ. The first and the second sums are over NN pairs. The exchange interaction with strength $J > 0$ is responsible for the superfluid ordering, while the random anisotropy Δ_i is related to the difference of chemical potentials $\mu_3 - \mu_4$ at site i, and $K = K_{33} + K_{44} - 2K_{34}$, where $K_{\alpha\beta}$ is the interaction energy between $^\alpha$He and $^\beta$He atoms. $K_{\alpha\beta}$ does not depend significantly on α and β and so it is generally assumed that $K = 0$.

Since we are going to study a model for ^{3}He–^{4}He mixtures in aerogel, we will let each Δ_i take the value Δ_0 or Δ_1 with the same meaning as in [1], i.e. $\Delta_0 < 0$ is the value of the anisotropy at the pore–grain interface of aerogel (where ^{4}He prefers to stay), while Δ_1 can be thought of as a bulk field which controls the ^{3}He concentration x.

As we mentioned in the introduction we take into account NN correlations in the random field distribution assuming the following joint probability density (with i and j NNs) for the Δ_i values:

$$P(\Delta_i, \Delta_j) = \sum_{n_1, n_2 = 0, 1} p_{n_1 n_2} \delta(\Delta_i - \Delta_{n_1}) \delta(\Delta_j - \Delta_{n_2}) \tag{2}$$

$$p_{n_1 n_2} = p_{n_1} p_{n_2} + (2\delta_{n_1 n_2} - 1)\epsilon p^2 \tag{3}$$

where $p_0 = p$ is the fraction of sites at the aerogel interface (the grain space is neglected), $p_1 = 1 - p$ and ϵ is a measure of the interface correlation. Integrating Δ_j one obtains

$$P(\Delta_i) = p\delta(\Delta_i - \Delta_0) + (1 - p)\delta(\Delta_i - \Delta_1) \tag{4}$$

which was used as a starting point in [1].

Two global order parameters can be defined in our model: $m = \langle\langle S_i\rangle\rangle_\Delta$ and $q = \langle\langle S_i^2\rangle\rangle_\Delta$, which are the quenched averages of the thermal equilibrium values $\langle S_i\rangle$ and $\langle S_i^2\rangle$. m is the superfluid order parameter, while $q = 1 - x$ is the ^{4}He concentration. Furthermore, we will also need the 'local order parameters'

$$\begin{aligned} m_n &= \frac{\langle\langle\delta(\Delta_i, \Delta_n)S_i\rangle\rangle_\Delta}{p_n} \qquad & m_{n_1n_2} &= \frac{\langle\langle\delta(\Delta_i, \Delta_{n_1})\delta(\Delta_j, \Delta_{n_2})S_i\rangle\rangle_\Delta}{p_{n_1n_2}} \\ q_n &= \frac{\langle\langle\delta(\Delta_i, \Delta_n)S_i^2\rangle\rangle_\Delta}{p_n} \qquad & q_{n_1n_2} &= \frac{\langle\langle\delta(\Delta_i, \Delta_{n_1})\delta(\Delta_j, \Delta_{n_2})S_i^2\rangle\rangle_\Delta}{p_{n_1n_2}} \end{aligned} \tag{5}$$

among which the following relations hold:

$$\begin{aligned} m &= \sum_n p_n m_n \qquad & p_n m_n &= \sum_{n'} p_{nn'} m_{nn'} \\ q &= \sum_n p_n q_n \qquad & p_n q_n &= \sum_{n'} p_{nn'} q_{nn'}. \end{aligned} \tag{6}$$

We are now ready to build the pair CVM free energy following the procedure outlined by Morita [9] for a general random system, which we briefly review.

Consider a random system on a finite lattice, for which the configuration of random fields and interactions is specified by a unique random variable h with distribution $P(h)$, and define, according to the usual rules of statistical mechanics, a density matrix $\rho_c(\sigma|h)$ for each configuration h (σ stands for the set of statistical degrees of freedom of the system, e.g. spin variables). In terms of ρ_c, the free energy associated with the configuration h will be given by

$$F(h) = \sum_\sigma \rho_c(\sigma|h)\,[H(h, \sigma) + k_B T \ln \rho_c(\sigma|h)] \tag{7}$$

where $H(h, \sigma)$ is the hamiltonian, k_B Boltzmann's constant, and T absolute temperature. The quenched free energy F will then be given by

$$F = \sum_h P(h)F(h). \tag{8}$$

Upon introducing the generalized density matrix

$$\rho(h, \sigma) = P(h)\rho_c(\sigma|h) \tag{9}$$

one can easily show that

$$F = \sum_{h,\sigma} \rho(h, \sigma)\,[H(h, \sigma) + k_B T \ln \rho(h, \sigma)] + TS_c \tag{10}$$

where S_c depends only on $P(h)$ and is given by

$$S_c = -k_B \sum_h P(h) \ln P(h). \tag{11}$$

As in the pure case, we have a variational principle: $\rho(h, \sigma)$ can be determined as the matrix that minimizes F, as given by (10), with the constraint

$$\sum_\sigma \rho(h, \sigma) = P(h). \tag{12}$$

In such a scheme it can be shown that the quenched average of the expectation value $\langle A(h, \sigma)\rangle$ of an operator $A(h, \sigma)$ is given by

$$\langle\langle A(h, \sigma)\rangle\rangle_h = \sum_h P(h)\langle A(h, \sigma)\rangle = \sum_{h,\sigma} \rho(h, \sigma) A(h, \sigma). \tag{13}$$

The CVM can then be obtained by taking the thermodynamic limit and truncating the cumulant expansion for the entropy $S = -k_B T \sum_{h,\sigma} \rho(h, \sigma) \ln \rho(h, \sigma)$ to a set of 'maximal preserved clusters' Γ_i, $i = 1, 2, \ldots, r$ (and all their translates). The variational principle will then be applied to the reduced density matrices $\rho_{\Gamma_i}(h, \sigma)$ associated with the maximal preserved clusters.

In the following, our maximal preserved cluster will be the NN pair, and thus we will introduce a density matrix ρ_p with elements $\rho_p(h, \sigma) \equiv \rho_p^{(n_1,n_2)}(S_1, S_2)$ ($n_1, n_2 = 0, 1$; $S_1, S_2 = \pm 1, 0$), where $h = (\Delta_{n_1}, \Delta_{n_2})$ is the random field configuration on the cluster and $\sigma = (S_1, S_2)$ denotes the set of spin variables. ρ_p (which is diagonal, since we are dealing only with the z component of the spins) is subject to the constraint $\sum_\sigma \rho_p(h, \sigma) = P(h)$, that is

$$\sum_{S_1 S_2} \rho_p^{(n_1,n_2)}(S_1, S_2) = p_{n_1 n_2}. \tag{14}$$

Writing ρ_p as a direct sum of density matrices, one for each possible configuration of the random fields on the cluster

$$\rho_p = \bigoplus_{n_1,n_2=0,1} p_{n_1 n_2} \tilde{\rho}_p^{(n_1,n_2)} \tag{15}$$

the constraint (14) becomes

$$\mathrm{Tr}\, \tilde{\rho}_p^{(n_1,n_2)} = 1 \qquad n_1, n_2 = 0, 1. \tag{16}$$

Furthermore, ρ_p has the obvious symmetry property

$$\rho_p^{(n_1,n_2)}(S_1, S_2) = \rho_p^{(n_2,n_1)}(S_2, S_1) \geqslant 0. \tag{17}$$

As usual, a (reduced) site density matrix can be obtained from ρ_p by a partial trace:

$$\rho_s = \mathop{\mathrm{Tr}}_{p\backslash s} \rho_p \tag{18}$$

or, more explicitly,

$$\rho_s^{(n_1)}(S_1) = \sum_{n_2 S_2} \rho_p^{(n_1,n_2)}(S_1, S_2). \tag{19}$$

The pair CVM free energy is then given by

$$F = U + k_B T \left[(1-\nu)\mathrm{Tr}(\rho_s \ln \rho_s) + \frac{\nu}{2}\mathrm{Tr}(\rho_p \ln \rho_p) \right] \tag{20}$$

with $U = \langle\langle H \rangle\rangle_\Delta$ and ν the coordination number of the lattice, and has to be minimized with respect to ρ_p, with the constraints (16) and (17). Taking derivatives of F with respect to ρ_p leads to three systems of equations, which are linear in the elements of $\ln \tilde{\rho}_p^{(00)}$, $\ln \tilde{\rho}_p^{(01)}$ and $\ln \tilde{\rho}_p^{(11)}$ respectively, and where the elements of $\ln \rho_s$ can be treated as parameters. Exponentiating the solution and making use of (16) yields

$$\rho_p^{(n_1,n_2)}(S_1, S_2) = p_{n_1 n_2} \frac{e^{(\beta/\nu) S_1 S_2} V_{S_1}^{(n_1)} V_{S_2}^{(n_2)}}{\sum_{S_1, S_2} e^{(\beta/\nu) S_1 S_2} V_{S_1}^{(n_1)} V_{S_2}^{(n_2)}} \tag{21}$$

with $\beta = \nu J / k_B T$ and

$$V_\pm^{(n)} = e^{-(\beta/\nu) d_n} \left[\frac{q_n \pm m_n}{2(1-q_n)} \right]^\alpha \qquad V_0^{(n)} = 1$$

where $\alpha = 1 - 1/\nu$, $d_n = \Delta_n/(\nu J)$. The parameters m_n and q_n, which have been defined in (5), are given by

$$\begin{aligned} m_n &= \tilde{\rho}_s^{(n)}(+) - \tilde{\rho}_s^{(n)}(-) \\ q_n &= \tilde{\rho}_s^{(n)}(+) + \tilde{\rho}_s^{(n)}(-). \end{aligned} \tag{22}$$

It can be easily shown that m_n and q_n are solutions of the following equations:

$$\begin{cases} p_n m_n = \sum_{n_2, S_2} \left(\rho_p^{(n,n_2)}(+, S_2) - \rho_p^{(n,n_2)}(-, S_2) \right) \\ p_n q_n = \sum_{n_2, S_2} \left(\rho_p^{(n,n_2)}(+, S_2) + \rho_p^{(n,n_2)}(-, S_2) \right) \end{cases} \tag{23}$$

which, together with (21), are the basic results of this section, and the starting point for the analysis of the phase diagram of our model at finite temperature.

3. The phase diagram

At zero temperature, several different phases can be found, which will be identified by the set ($m_{00} = q_{00}, m_{01} = q_{01}, m_{10} = q_{10}, m_{11} = q_{11}$), obtainable by the relations

$$\begin{aligned} m_{n_1 n_2} &= \sum_S \left(\tilde{\rho}_p^{(n_1,n_2)}(+, S) - \tilde{\rho}_p^{(n_1,n_2)}(-, S) \right) \\ q_{n_1 n_2} &= \sum_S \left(\tilde{\rho}_p^{(n_1,n_2)}(+, S) + \tilde{\rho}_p^{(n_1,n_2)}(-, S) \right). \end{aligned} \tag{24}$$

The phase diagram is easily determined by comparing the energies U of the different phases, and is reported in figure 1. Two comments are in order: (i) as opposed to the mean-field result [1], the boundaries between the different ground states no longer depend on the probability distribution of the random variables and (ii) increasing the level of the approximation we have obtained a more complicated phase diagram, with a larger number of possible ground states. This is reminiscent of what happens in the exact solution at $T = 0$ of the random-field Ising model on a Bethe lattice [11]. Notice that our model (1) reduces to a random-field Ising model for $J = 0$ and $K \neq 0$ since all spin variables appear squared and thus assuming only the two values zero and unity.

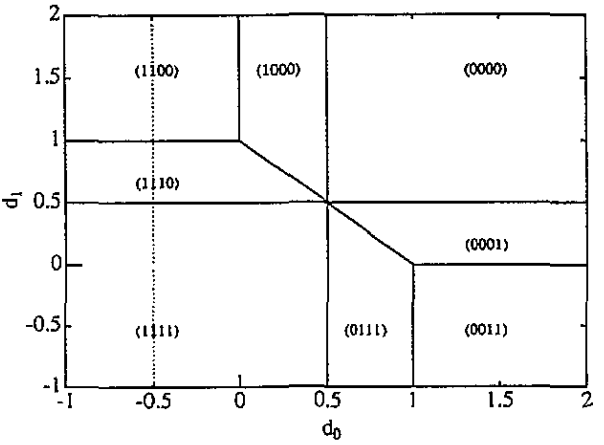

Figure 1. Phase diagram at $T = 0$.

At finite temperature, and for $\Delta_0 < 0$, it has been shown in the mean-field analysis [1] that the phase diagram has quite a rich structure, with a second-order transition separating the ordered phases from the disordered one, a first-order transition, terminating in a critical point, between the ordered phases above, and several multicritical points. Our approximation yields an even richer structure: indeed we have three different ground states (see the dotted line in figure 1), (1111) for $d_1 < \frac{1}{2}$ corresponding to ^{4}He present everywhere, (1110) for $\frac{1}{2} < d_1 < 1$, which corresponds to ^{4}He present in the aerogel interface and in its neighbourhood, i.e. everywhere except in the bulk of the pore space† and (1100) for $d_1 > 1$, i.e. ^{4}He only at the aerogel interface. Again, ordered phases are separated by the disordered (high-temperature) one by a second-order transition line, for which an equation can be obtained by expanding (23) around $m_0 = m_1 = 0$. Up to the first order, the equations for m_n yield

$$\begin{cases} m_0 = a_{00}m_0 + a_{01}m_1 \\ m_1 = a_{10}m_1 + a_{11}m_1 \end{cases} \tag{25}$$

where

$$a_{\gamma\lambda} = \alpha\left[\delta_{\gamma\lambda} + 4\frac{p_{\gamma\lambda}}{p_\gamma q_\lambda}\frac{V^{(\gamma)}V^{(\lambda)}}{Z_{\gamma\lambda}}\sinh\frac{\beta}{\nu}\right]. \tag{26}$$

† Notice that m_{11} as a 'local order parameter' is averaged only over pore–pore pairs.

The equation for the critical temperature turns out to be

$$(a_{00} - 1)(a_{11} - 1) = a_{01}a_{10} \tag{27}$$

meaning that a non-trivial solution of (25) exists, where q_0 and q_1 must be determined from the corresponding equations with $m_0 = m_1 = 0$. A solution for the critical temperature is obtained for $d_1 \to +\infty$ (and thus for any d_1) only if p is greater than the percolation threshold p_c.

The percolation threshold can be defined as follows: in the limit $\Delta_1 \to +\infty$, S_i will be 0 for all sites with anisotropy Δ_1 and our model will be equivalent to a random-diluted BEG model with anisotropy Δ_0 and concentration p, corresponding to a situation with all the ^{4}He at the aerogel interface and all the ^{3}He in the pore space. Such a model will undergo a second-order transition at $T_c > 0$ for any large enough p, and the percolation threshold is simply that value of p for which T_c becomes zero. For $p > p_c$ a macroscopic, infinite cluster of sites with anisotropy Δ_0 will form, making long-range order possible.

p_c can be obtained by taking the limits $\Delta_1 \to +\infty$ and $\beta \to +\infty$ in the equation for the critical temperature, and the result is

$$p_c = \frac{1}{(\nu - 1)(1 + \epsilon)} \tag{28}$$

representing a remarkable improvement with respect to the mean-field theory, which gives $p_c = 0$. Notice that for uncorrelated disorder, i.e. $\epsilon = 0$, the exact result for the Bethe lattice with coordination ν is recovered [12].

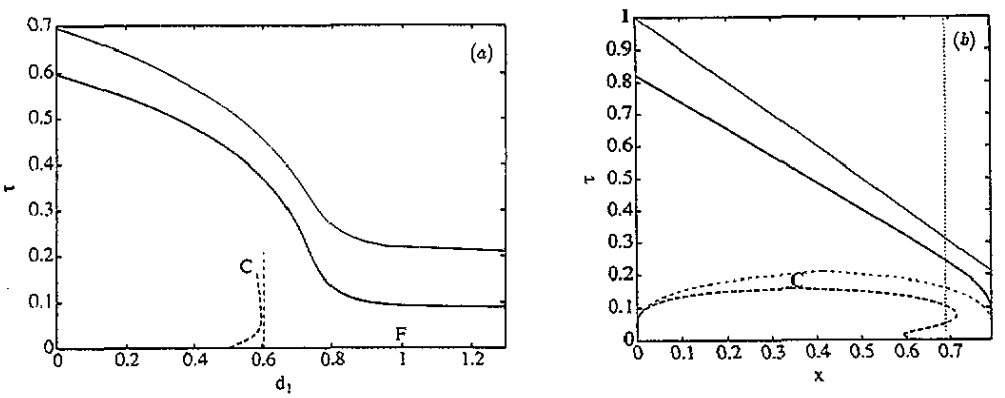

Figure 2. (*a*) Phase diagram in the (d_1, τ) plane for $\nu = 6$, $\epsilon = 0$, $p = 0.21 > p_c$, $d_0 = -0.5$. Heavy lines are our results and light lines are results from the mean-field approximation. (*b*) Phase diagram in the (x, τ) plane for the case of (*a*). Symbols as in (*a*) (for the dotted line see figure 6).

For $p > p_c$ the phase diagram has the structure shown in figure 2 (heavy lines): solid lines are used for the second-order transition, while dashed lines stand for the first-order transition separating (1111) and (1110) phases (if in the $(d_1, \tau = \beta^{-1})$ plane) or for the corresponding coexistence region (if in the (x, τ) plane, where x is the ^{3}He concentration). C is a critical point. No first-order line separating (1110) and (1100) phases seems to start from the point $F(d_1 = 1, \tau = 0)$, where a first-order transition occurs at zero temperature.

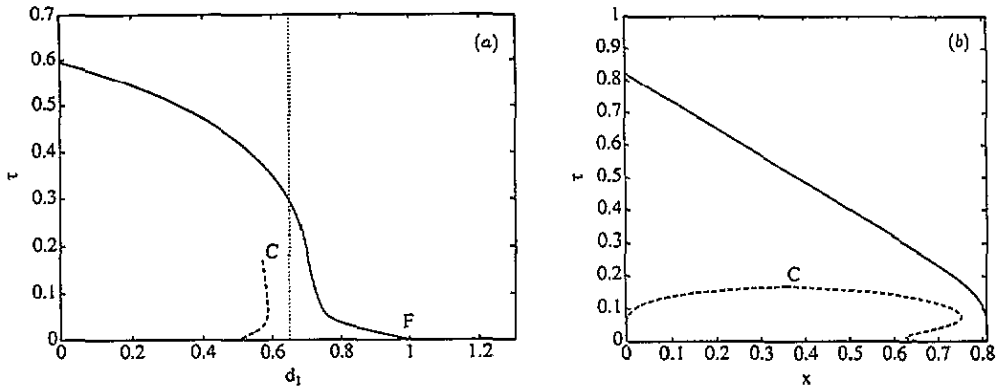

Figure 3. (*a*) The same as figure 2(*a*) with $p = 0.19 < p_c$ (for the dotted line see figure 5). (*b*) Phase diagram in the (x, τ) plane for the case of (*a*).

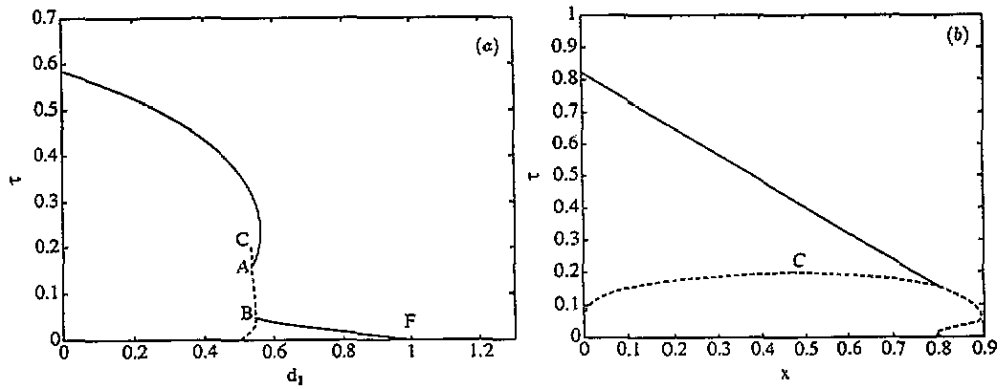

Figure 4. (*a*) The same as figure 2(*a*) with $p = 0.1 < p_c$. (*b*) Phase diagram in the (x, τ) plane for the case of (*a*).

Again this is reminescent of the behaviour of the random-field Ising model on the Bethe lattice [11]. The phase diagram at $T > 0$ is qualitatively the same as that given by mean-field theory, which is reported for comparison (light lines). In all cases considered ($\Delta_0 < 0$) $x < 1 - p$.

For $0 < p < p_c$ a new feature arises that cannot be described by mean-field theory: the second-order line has a limit point F at zero temperature and $d_1 = 1$, independent of p, ϵ and d_0, and the critical temperature is zero for any $d_1 > 1$, meaning that, even if the ground state is ordered, the aerogel concentration is too low for the pore–grain interface to sustain an ordered phase at finite (i.e. non-zero) temperature. The corresponding phase diagrams are given in figure 3 and in figure 4, for typical values of the parameters. In the latter case the second-order line is reentrant and intersects the first-order line in the critical end points A and B. C is again a critical point which, together with the critical end point A, belongs to an 'internal critical-end-point' structure such as that studied, e.g. by Netz and Berker [13] for the pure model. It is easily realized that there exists a value $p^* < p_c$ of p for which the points A and B merge into one, giving rise to a new multicritical point where the second- and the first-order lines are tangential to each other. It is also interesting to remark that the

first-order transition always has a reentrant behaviour, a feature that does not exist in the mean-field treatment [1].

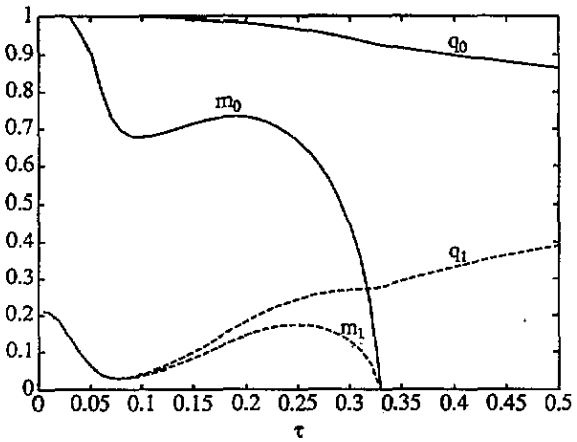

Figure 5. m_n and q_n versus τ along the dotted line in figure 3(a) ($d_1 = 0.65$).

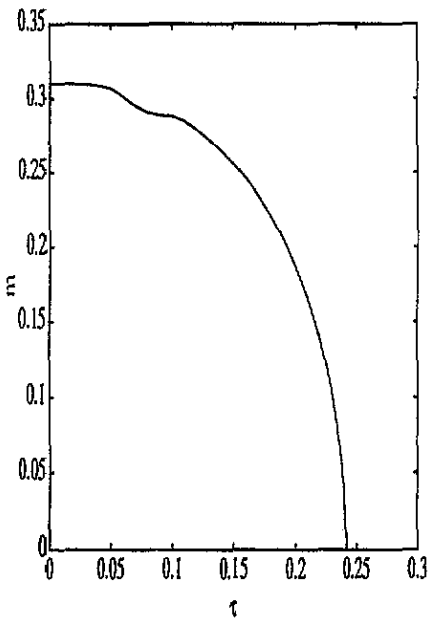

Figure 6. m versus τ along the dotted line in figure 2(b) ($x = 0.69$).

In our scheme the behaviour of order parameters and NN correlation functions can be obtained in a natural way: in figure 5 we report the behaviour of the local order parameters m_n and q_n versus temperature for the case $\frac{1}{2} < d_1 < 1$ (dotted line in figure 3(a)), where $m_0 = q_0 = 1$ and $m_1 = q_1 = p_{10}/(1-p)$ in the ground state. It is interesting that m_0 and m_1 exhibit a quite unusual oscillation. The increase at intermediate temperatures might be due to the reentrant behaviour of the first-order line, so that the completely ordered (1111)

phase becomes closer as the temperature is raised along the dotted line. Furthermore, in figure 6, we report the global order parameter m versus temperature at fixed concentration, corresponding to the dotted line in figure 2(b).

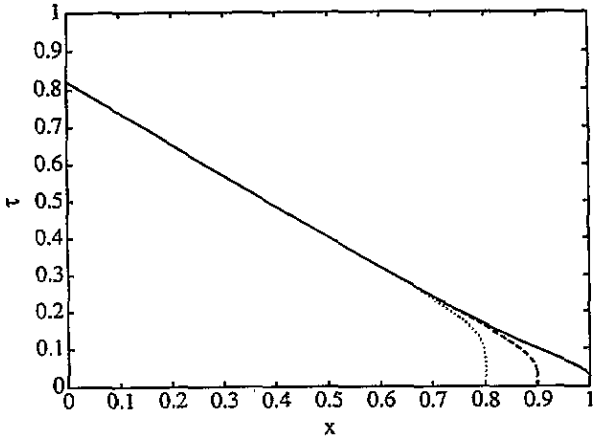

Figure 7. The critical temperature in the (x, τ) plane for $\nu = 6$, $\epsilon = 0$, $d_0 = -0.5$ and $p = 0$ (solid line), 0.1 (dashed line) and 0.2 (dotted line).

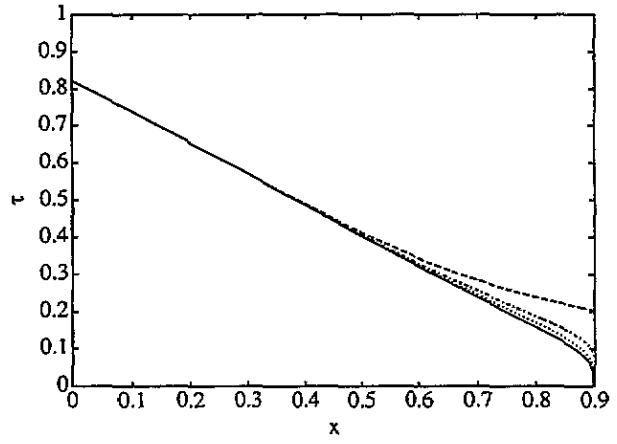

Figure 8. The critical temperature in the (x, τ) plane for $\nu = 6$, $d_0 = -0.5$, $p = 0.1$ and $\epsilon = 0$ (solid line), 0.5 (dotted line), 1.0 (dot–dashed line) and 2.0 (dashed line).

Finally, let us discuss the effect of a correlation $\epsilon > 0$ in the random distribution on the phase diagram, and especially on the second-order transition. In the mean-field analysis [1] it was shown that the second-order transition occurs at $\tau = 1 - x = q$, independent of p, while our analysis shows that the second-order critical temperature at fixed concentration is indeed weakly dependent on p (figure 7). Introducing a correlation ϵ of order unity in the random distribution of the Δ_i values causes the critical temperature to increase significantly,

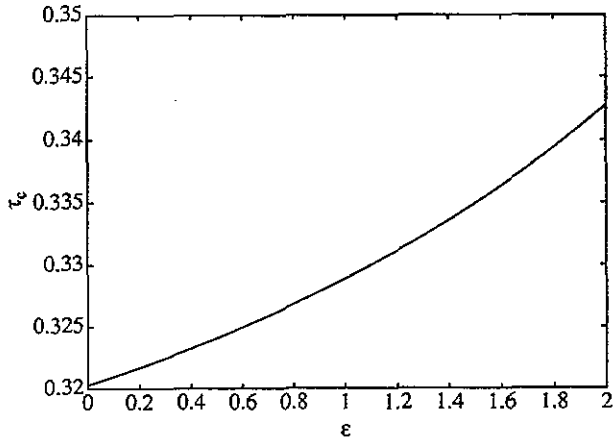

Figure 9. The critical temperature versus ϵ for the case of figure 7 and with $x = 0.6$.

especially in the low-q (high-x) region (figure 8), and we believe that this effect should account for the experimentally observed [7] increase in the critical temperature with respect to the pure case. The behaviour of T_c as a function of ϵ is shown in figure 9.

4. Conclusions

A model for the critical behaviour of ^{3}He–^{4}He mixtures in a porous medium (aerogel), namely the random-anisotropy Blume–Emery–Griffiths model [1], has been investigated in the pair approximation of the cluster variation method. This improves the mean-field analysis given in [1] in several directions. A rather rich phase diagram is found even at zero temperature, with various ground states corresponding to $\Delta_0 < 0$: ^{4}He present everywhere, (1111) in figure 1, at the aerogel interface and in its neighbourhood (1110), and only at the aerogel interface (1100). The symmetric situations, with ^{3}He preferentially near aerogel, are of course possible within the context of a model (figure 1 for $d_0 > \frac{1}{2}$).

A non-zero percolation threshold can be determined, above which the phase diagram is mean field like, and below which it changes qualitatively, with the appearance of a zero-temperature limit point for the second-order transition line. A completely open and extremely interesting question concerns the universality class of the whole line of continuous transitions: is there a zero temperature or $d_1 = +\infty$ fixed point attracting a finite part of the critical line and an unstable fixed point at finite temperature separating two different critical behaviours (e.g. $d_1 < 0$ and $d_1 \simeq 1$)? A real-space renormalization group analysis might be suitable to address this problem.

In all considered cases, the first-order transition line (in the temperature–anisotropy phase diagram) and the coexistence region (in the temperature–concentration phase diagram) exhibit reentrant behaviour. This reentrance is also partially responsible for the existence of a miscibility gap on the high-^{3}He-concentration side going down to zero temperature.

The experimental phase diagrams are in remarkable agreement with those presented in figures 2(b) and 3(b). Quantitative comparisons would of course require more adequate treatments of the superfluid transition.

Particular attention has been devoted to the analysis of the effects of a nearest-neighbour correlation in the random distribution of the anisotropy, which should not be neglected due

to the high correlation characterizing the aerogel interface. The main result is the increase in the critical temperature with respect to the pure case, contributing to the detachment of the λ line from the coexistence curve, which has been experimentally observed [7] and cannot be explained in terms of uncorrelated randomness alone. Correlations in the quenched impurities make the question of the universality class of the critical line more involved even at low disorder concentration.

Acknowledgments

We are indebted to Jayanth Banavar, Moses Chan and Flavio Toigo for enlighting discussions. We also thank Moses Chan for sending us the results of [7] before publication.

References

[1] Maritan A, Cieplak M, Swift M R, Toigo F and Banavar J R 1992 *Phys. Rev. Lett.* **69** 221
[2] Fricke J 1988 *Sci. Am.* **258** 92
[3] Tillotson T M, Hrubesh L W and Thomas I M 1988 *Better Ceramic through Chemistry III (Mater. Res. Soc. Symp. Proc.* vol 121 ed C Brinker, D Clark and D Ulrich (Pittsburgh, PA: Materials Research Society) p 685
[4] Schaefer D W, Brinker C J, Richter D, Farago B and Frick B 1990 *Phys. Rev. Lett.* **64** 2316
[5] Wong A 1991 *PhD Thesis* Penn State University
[6] Blume M, Emery V J and Griffiths R B 1971 *Phys. Rev.* A **4** 1071
[7] Ma J, Kim S and Chan M H W in preparation
[8] Kikuchi R 1951 *Phys. Rev.* **81** 988
An G 1988 *J. Stat. Phys.* **52** 727
Morita T 1990 *J. Stat. Phys.* **59** 819
[9] Morita T 1984 *Prog. Theor. Phys. Suppl.* **80** 103
See also Falk H 1976 *J. Phys. C: Solid State Phys.* **9** L213
[10] de Smedt Ph, Indekeu J O and Zhang L 1987 *Physica* A **140** 450
[11] Bruinsma R 1984 *Phys. Rev.* B **30** 289
[12] Fisher M E and Essam J W 1961 *J. Math. Phys.* **2** 609
[13] Netz R R and Berker A N 1993 *Phys. Rev.* B **47** 15019